PNAS RESEARCH ARTICLE | NEUROSCIENCE

Anion efflux mediates transduction in the hair cells of the zebrafish lateral line

Elias T. Lunsford[a,b,1], Yuriy V. Bobkov[a,1], Brandon C. Ray[a], James C. Liao[a,2], and James A. Strother[a,2]

Edited by A. Hudspeth, The Rockefeller University, New York, NY; received September 6, 2023; accepted November 1, 2023

Hair cells are the principal sensory receptors of the vertebrate auditory system, where they transduce sounds through mechanically gated ion channels that permit cations to flow from the surrounding endolymph into the cells. The lateral line of zebrafish has served as a key model system for understanding hair cell physiology and development, often with the belief that these hair cells employ a similar transduction mechanism. In this study, we demonstrate that these hair cells are exposed to an unregulated external environment with cation concentrations that are too low to support transduction. Our results indicate that hair cell excitation is instead mediated by a substantially different mechanism involving the outward flow of anions. Further investigation of hair cell transduction in a diversity of sensory systems and species will likely yield deep insights into the physiology of these unique cells.

sensory transduction | hair cells | auditory | vestibular | chloride

Vertebrate hair cells are ciliated mechanoreceptive sensory cells responsible for the exquisite sensitivity of the auditory and vestibular systems. In the auditory system, these cells are immersed in endolymph with a relatively high K^+ concentration and positive potential, which establishes a strong electrochemical gradient favoring K^+ influx into the cells (1–3). Sound propagating through the cochlea generates shearing forces on the apical stereocilia bundle of hair cells. Deflection of the stereocilia opens mechanically gated cation channels [i.e., TMC1/2; (4–6)], which permits K^+ influx into the hair cells [mechanoelectrical transduction (MET) current] and drives membrane depolarization (7, 8). The high K^+ concentration of the endolymph is key to this pathway and is produced by active secretion of K^+ into the endolymph by strial marginal cells via a process that includes K^+ channels and Na^+/K^+ ATPase (9–11).

The hair cells of the inner ear are thought to have evolved from anatomically similar cells found in the lateral line of fishes and amphibians (reviewed by ref. 12). The lateral line system detects the movement of water around the body and is critical for survival, as it mediates behaviors such as predator avoidance, prey capture, and navigation (13–16). Unlike the hair cells of the inner ear, the lateral line hair cells lie on the surface of the body and are typically surrounded by a potentially unstable external environment rather than a regulated, K^+-rich endolymph. Work in amphibians in the 1970s indicated that the gelatinous cupula that partially encapsulates the lateral line hair cells maintains an ionic microenvironment comparable to the inner ear endolymph, which establishes the ionic gradient necessary for cation influx–mediated mechanotransduction (17, 18). It has often been assumed that a similar mechanism is responsible for mechanotransduction in other aquatic organisms, including freshwater fishes.

Although the lateral line of freshwater zebrafish is a powerful model system for understanding hair cell physiology (19–21), this foundational hypothesis has remained largely untested. Here, we show that the ionic microenvironment in the cupula of the superficial neuromasts of zebrafish larvae is indistinguishable from the surrounding freshwater. Electrochemical calculations indicate that the freshwater inhabited by zebrafish does not provide ionic gradients sufficient to support the putative cation-mediated mechanotransduction mechanism. Instead, our results suggest an alternative process driven by anion efflux. For cells in contact with ion-poor extracellular saline, typical negative resting membrane potentials and intracellular Cl^- concentrations are sufficient to generate anion efflux capable of inducing robust membrane depolarization. Although studies of sensory physiology often focus on cation-mediated transduction process, anion efflux has been observed to contribute to signal amplification in vertebrate chemosensory receptors, which often directly interface with an unregulated external environment (22–26). It has also been argued that anion efflux may confer favorable properties, including reduced sensitivity to large variations in extracellular ionic composition (27, 28).

Significance

Hair cells in vertebrates are specialized sensory cells with a central role in hearing, balance, and flow sensing. The process by which hair cells transduce mechanical stimuli has been the subject of intense study, frequently with the implicit assumption that hair cells in different sensory systems and across species employ a similar transduction mechanism. Here, it is shown that the hair cells of the zebrafish lateral line system use a substantially different mechanism driven by the efflux of anions rather than the influx of cations. These results establish a new perspective for examining the physiology and evolution of hair cells and other sensory cells.

Author affiliations: [a]Department of Biology, The Whitney Laboratory for Marine Bioscience, University of Florida, Saint Augustine, FL 32080; and [b]Institut du Cerveau (Paris Brain Institute), Hôpital Pitié-Salpêtrière, Paris 75013, France

Pre-Print Servers: BioRxiv (https://doi.org/10.1101/2022.07.11.499370).

Author contributions: E.T.L., Y.V.B., J.C.L., and J.A.S. designed research; E.T.L., Y.V.B., B.C.R., J.C.L., and J.A.S. performed research; E.T.L., Y.V.B., B.C.R., J.C.L., and J.A.S. analyzed data; and E.T.L., J.C.L., and J.A.S. wrote the paper.

The authors declare no competing interest.

This article is a PNAS Direct Submission.

[1]E.T.L. and Y.V.B. contributed equally to this work.

[2]To whom correspondence may be addressed. Email: james.strother@whitney.ufl.edu or jliao@whitney.ufl.edu.

This article contains supporting information online at https://www.pnas.org/lookup/suppl/doi:10.1073/pnas.2315515120/-/DCSupplemental.

Published December 20, 2023.

Results

The Cupula Does Not Provide a Cation-Rich Microenvironment for Lateral Line Hair Cells. We first examined whether the cupula of the superficial neuromasts contained an elevated K^+ concentration capable of supporting mechanotransduction. Animals were bathed in a freshwater medium (E3 saline) with a K^+ selective fluorescent indicator (IPG-4). Using confocal microscopy, we found that fluorescence in the cupula was nearly indistinguishable from that of the surrounding water, suggesting that the cupula does not maintain elevated K^+ concentrations (Fig. 1 *A* and *B*). To quantify the K^+ concentration within the cupula, the indicator was saturated by adding K^+ to the surrounding medium, and the recorded fluorescence values were fit to a model that incorporates both the binding affinity of the indicator and potential differences in indicator concentration between the cupula and medium. Consistent with our qualitative observations, the calculated K^+ concentration of the cupula was not significantly different from that of the surrounding medium (P = 0.26, N = 11; Fig. 1*C*). Analogous experiments were then performed examining each of the major cations present in freshwater saline and again no significant differences were found between the cupula and the surrounding water (Na^+: P = 0.88, N = 8; Ca^{2+}: P = 0.45, N = 9; H^+: P = 0.30, N = 8; Fig. 1*D*). We also examined the Cl^- concentration within the cupula, since it is the likely counterion for any cation, and found that it was also not significantly different from the freshwater medium (P = 0.43, N = 6, Fig. 1*D*). These results indicate that the cupula does not support an ionic microenvironment, and the apical surfaces of the lateral line hair cells are directly exposed to an ion-poor freshwater saline that is markedly different from the endolymph of the inner ear (2, 3, 29–31).

To systematically explore the consequences of the hair cells being exposed to an ion-poor environment, we calculated the membrane reversal potential for a MET channel in different extracellular solutions, assuming relative permeabilities similar to other hair cells (*SI Appendix, Membrane Reversal Potentials*). We found that in a freshwater medium (E3 saline), MET conductance would be expected to produce K^+ efflux and hyperpolarization rather than depolarization, which suggests that K^+ current is not the primary driver of transduction (Fig. 1*E*). MET conductance is only predicted to induce membrane depolarization sufficient to open the voltage-gated Ca^{2+} channels on the basolateral membrane [$Ca_V1.3$, (32)] in water with cation concentrations much greater than those in the natural habitat of zebrafish [Fig. 1*E*, (29–31)]. Although the chemical gradient favors Ca^{2+} influx into the hair cell, this influx is unable to overcome the hyperpolarizing effect generated by K^+ efflux given the estimated relative permeabilities of the MET channels. Ca^{2+} currents would therefore only be sufficiently depolarizing if the MET channels displayed Ca^{2+} selectivity far in excess of that reported in other systems (4). We next calculated the reversal potential for a hypothetical Cl^- channel and found that Cl^- conductance would be expected to readily drive Cl^- efflux from the hair cells and membrane depolarization in a wide range of external environments (Fig. 1*E*). In total, these results argue against K^+ influx as a mechanism for lateral line hair cell depolarization and suggest that Ca^{2+} influx or Cl^- efflux may have more central roles.

The lack of an ionic microenvironment in the cupula would profoundly affect the mechanotransduction mechanisms available to hair cells. We next conducted a series of experiments and simulations further exploring whether the physical properties of the cupula could support such a microenvironment. We first examined the diffusion of charged molecules within the cupula by rapidly introducing a negatively charged small molecule fluorophore

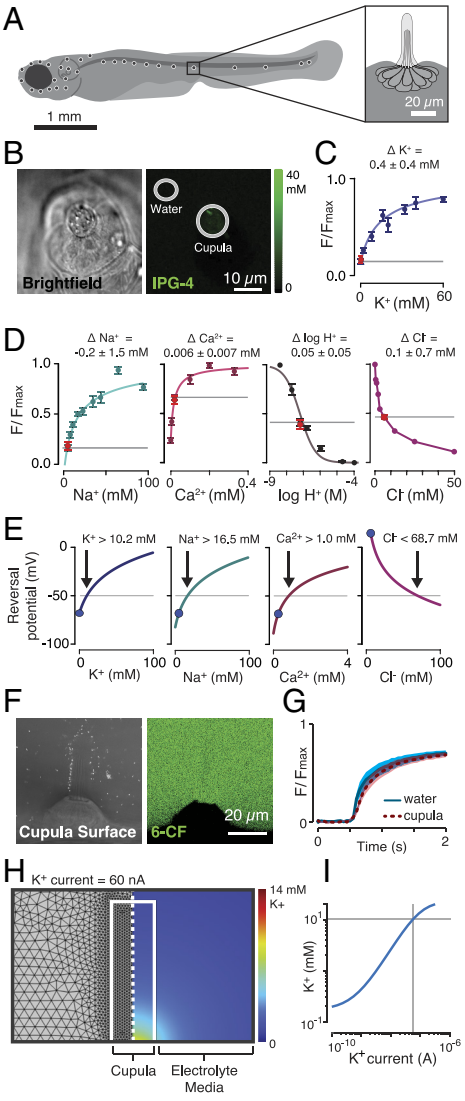

Fig. 1. The ionic microenvironment of the cupula resembles freshwater and cannot support cation influx–mediated depolarization. (*A*) Superficial neuromasts of the lateral line system in larval zebrafish. (*B*) In vivo visualization of K^+ in the vicinity of a neuromast using the fluorescent probe IPG-4 (*Left*: brightfield; *Right*: IPG-4). (*C*) Fluorescence of K^+ probe in solutions with varying K^+ concentrations (blue, error bars are ± SEM, curve is fit model), fluorescence expected for an environment matching the surrounding freshwater medium (E3 saline; horizontal gray line), and measured fluorescence within the cupula (red dot, error bars are ± SEM, error bars are small and may be partially obscured). The similarity of the cupula fluorescence (red dot) and freshwater medium fluorescence (gray line) suggests the K^+ concentration in the cupula is similar to the surrounding medium. Using these measured values, the difference between the K^+ concentration in the cupula and the surrounding medium was also calculated (ΔK^+, mean ± SEM). (*D*) Results from experiments similar to (*C*) except examining Na^+ (probe: ING-2), Ca^{2+} (probe: Fluo-5 N), H^+ (probe: BCECF), and Cl^- (probe: MQAE). In all cases, ion concentrations within the cupula matched those of the surrounding medium. (*E*) Predicted reversal potentials for MET channels as a function of cupula cation concentration. The estimated opening potential of voltage-gated Ca^{2+} channels at the basal membrane is indicated (−50 mV, horizontal line). The cation concentration necessary to reach this potential (black arrow) and the concentration in a freshwater medium (blue dot) are also indicated. The predicted reversal potential for a hypothetical chloride channel is also shown (right). (*F*) Images showing penetration of a charged fluorophore (6-carboxyfluorescein, 6-CF) into neuromast cupula (*Left*: cupula surface visualized with microspheres, *Right*: 6-CF). (*G*) From the same experiments as (*F*), time series showing rapid increase in fluorescence in both the medium around the cupula and within the cupula after introduction of the charged fluorophore. (*H*) Simulation of a hypothetical K^+ microenvironment, produced by solving 3D Nernst-Plank equations (*Left*: mesh, right: K^+ distribution for K^+ current = 60nA). (*I*) K^+ concentration at apical surface of hair cells as a function of K^+ secretion current [horizontal gray line: estimated K^+ concentration necessary for depolarization (10.2 mM), vertical gray line: corresponding K^+ efflux current (56 nA)].

(6-carboxyfluorescein; 6-CF) around the cupula and imaging its diffusion from the medium into the cupula (Fig. 1*F*). There were no significant differences between the rate at which fluorescence increased in the cupula and the surrounding water, suggesting that charged molecules rapidly penetrate the cupula [relative time constant = 0.88 ± 0.06 (mean ± SEM), $P = 0.076$, N = 9, Fig. 1*G*]. Computational simulations confirmed that this experimental setup had sufficient resolution to detect meaningful differences in the diffusive properties of the cupular matrix (*SI Appendix*, Fig. S1 *A–C*). This finding is also consistent with empirical studies of the ultrastructure of lateral line cupulae, which identified no membrane or other dense surface structure (33, 34).

We next evaluated the ion currents that would be necessary to sustain a K^+ reservoir in the cupula using computational simulations. Since this configuration violates the assumptions of a typical neuron electrical equivalent circuit (35), we simulated these dynamics by directly solving the full three-dimensional Nernst–Planck equations using the finite element method (Fig. 1*H*). Based on the above diffusion experiments, we estimated the diffusion coefficients for ions moving through the cupular matrix to be similar to that of water and assumed a constant rate of K^+ secretion into the matrix at the base of the neuromast. We found that a K^+ current of 56 nA would be needed to produce the K^+ concentration of 10.2 mM required for depolarizing MET conductance (Fig. 1 *E* and *I*). Although the ionoregulatory currents of the neuromast have not been quantified, these K^+ current values are several orders of magnitude greater than the resting MET current of hair cells (36, 37). These results indicate that recently described skin-derived ionocytes are unlikely to maintain a K^+ microenvironment at the apical surface of the hair cells but may instead support regulation of the extracellular environment at the basolateral surfaces (38).

Cumulatively, these experiments indicate that the cupula does not maintain a cation-rich microenvironment sufficient to support hair cell depolarization, challenging a long-standing assumption that hair cell transduction is cation driven in the lateral line system of zebrafish and other freshwater fishes.

Lateral Line Function Only Requires Micromolar Extracellular Calcium. What other mechanisms could mediate hair cell depolarization? We next tested the hypothesis that Ca^{2+} could contribute to hair cell depolarization, given its reversal potential and assuming MET channels with unusually high Ca^{2+} selectivity. Hair cells expressing the fluorescent calcium indicator GCaMP6s were imaged while mechanically deflecting the cupula with a piezoelectric transducer (Fig. 2*A*). Changes in fluorescence near the basal surface of the hair cells were observed, which have been attributed to Ca^{2+} influx through voltage-gated channels on the basal membrane (21). Hair cells produced robust responses to this stimulus in a freshwater medium (E3 saline, 330 μM Ca^{2+}; $P < 0.001$, df = 27; Fig. 2*A*). Interestingly, we found that hair cells continue to respond in a medium with substantially reduced Ca^{2+} concentrations (20 μM Ca^{2+}; $P = 0.04$, df = 3; Fig. 2*A*) and that these responses were indistinguishable from those observed in freshwater saline ($P = 0.13$, df = 3). The insensitivity of hair cell responses to the extracellular Ca^{2+} concentration may suggest that Ca^{2+} current is not crucial for mechanotransduction. However, responses in 0 μM Ca^{2+} medium were significantly reduced compared to those in freshwater saline ($P = 0.02$, df = 9; Fig. 2*A*). This indicates that environmental Ca^{2+} modulates MET currents in naturalistic freshwater media, consistent with observations in zebrafish and other species (8, 39–43).

To further examine the role of Ca^{2+} currents in hair cell depolarization, we used the Nernst–Planck computational model to

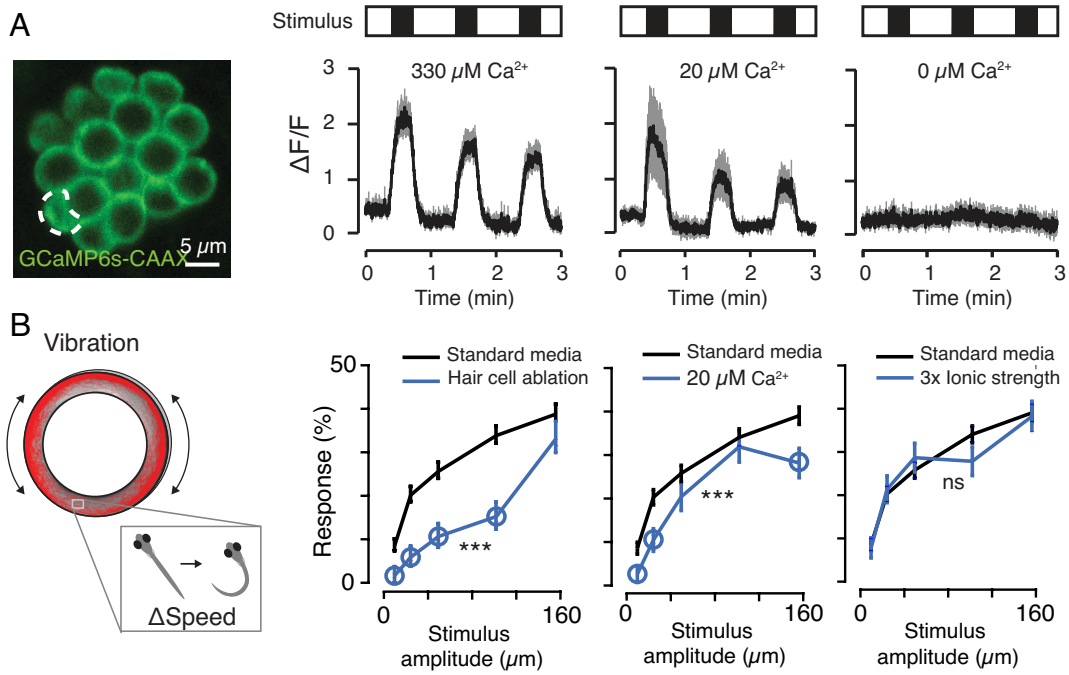

Fig. 2. Only micromolar extracellular calcium is required for lateral line function. (*A*) Response of hair cells to a mechanical stimulus, recorded by imaging genetically expressed fluorescent calcium indicator GCaMP6s-CAAX at the basal membrane (*Left*: typical image, region of interest indicated; *Right*: responses in 330 μM, 20 μM, and 0 μM Ca^{2+}, mean ± SEM). Hair cell responses in micromolar Ca^{2+} medium are comparable to those in a freshwater medium (E3 saline), while responses are abolished in a calcium-free medium. (*B*) Behavioral response of zebrafish larvae to a mechanical stimulus under varying conditions, recorded with a unique behavioral assay that employs an oscillatory Couette cell to produce a pure-shear flow stimulus (*Left*: schematic of behavioral setup with typical trajectory in red; *Right*: probability of response following neomycin-induced hair cell ablation, in 20 μM Ca^{2+} medium, and in 3× ionic strength medium). Asterisks indicate statistically significant differences integrated across stimulus intensities (*$P < 0.05$, **$P < 0.01$, ***$P < 0.001$), open circles represent significant pairwise comparisons ($P < 0.05$), and results are shown as mean ± SEM.

estimate the maximum sustainable Ca^{2+} current in the reduced Ca^{2+} medium (20 μM). We simulated a scenario where the stereocilia tips have infinite Ca^{2+} conductance, and the total Ca^{2+} current is limited by the diffusion of Ca^{2+} through the surrounding medium (*SI Appendix*, Fig. S1*D*). Using this approach, the maximum Ca^{2+} current into an isolated hair cell was estimated to be 2.8 pA, which is orders of magnitude smaller than a typical MET current (36, 37). These results indicate that the reduced Ca^{2+} medium cannot support large Ca^{2+} currents and provides further evidence that Ca^{2+} current is not critical to mechanotransduction. These findings do not rule out that possibility that Ca^{2+} current contributes to mechanotransduction in media with higher Ca^{2+} concentrations.

We next examined whether these cellular-scale differences were reciprocated at the organismal level by recording the effects of low Ca^{2+} environments on the behavior of freely swimming larvae. A number of behavioral assays have been successfully employed for assessing lateral line function in zebrafish larvae, including assays measuring C-start escapes in response to impulsive stimuli and assays measuring rheotactic responses (13–15). However, the contribution of multiple sensory modalities (e.g., vestibular, acoustic, visual) to behavioral responses often presents a challenge when developing such assays. Since the superficial lateral line is principally sensitive to shear at the body surface (44), we designed a novel behavioral assay that uses an oscillatory Couette cell to produce a shearing flow without accompanying pressure waves (*SI Appendix*, Fig. S2). The position and swimming speed of animals were continuously monitored, and stimuli of varying intensities were presented at random intervals. Each stimulus that produced a significant change in swimming speed (outside 95% CI) was recorded and then the net response probability was calculated as a function of stimulus intensity. In order to reduce both habituation and activation of collateral sensory modalities, we intentionally examined small stimulus intensities that produced modest changes in behavior with relatively low response probabilities rather than escape responses with high probability.

To evaluate the efficacy of this assay, we confirmed that animals responded in an intensity-dependent manner and that neomycin-induced hair cell ablation dramatically decreased this response (Fig. 2*B*). Next, we examined how low environmental Ca^{2+} affects lateral line sensitivity and found that animals displayed reduced but robust responses even with Ca^{2+} decreased by >15× (21% decrease with 50 μm stimulus, omnibus $P < 0.001$, N = 30 exp/94 ctrl). These results are consistent with our imaging data and data from other species (39, 45). Using this same assay, we then examined how lateral line sensitivity is altered by increases in the ionic strength of the freshwater environment. The responses of animals in a medium with a 3× increase in ionic strength were not significantly different from those in a freshwater medium (E3 saline, omnibus $P > 0.05$, N = 30 exp/94 ctrl). Media with higher ion concentrations were also explored, and significant decreases in sensitivity were detected, but such ion concentrations far exceed the values observed in the natural habitat of zebrafish and these effects may result from osmotic stress rather than a specific interaction with the lateral line (*SI Appendix*, Fig. S3). In total, these findings suggest that extracellular Ca^{2+} modulates the mechanotransduction process but does not provide the primary ion current driving hair cell depolarization.

Calcium-Activated Anion Efflux Contributes to Hair Cell Depolarization. Since the electrochemical gradient between hair cells and freshwater strongly favors anion efflux, we next examined whether this efflux could be contributing to mechanotransduction. We began by leveraging available transcriptome data to generate testable hypotheses. We analyzed published transcriptome scRNA-seq data collected from zebrafish lateral line neuromasts (46) for cells that expressed a hair cell marker (tmc2b), filtered transcripts for genes associated with ion channel activity, and then reviewed the resulting list for genes with anion efflux activity. This analysis indicated that the lateral line hair cells may express the calcium-activated anion channel Anoctamin-2b (ANO2b), also known as TMEM16b (Fig. 3*A*).

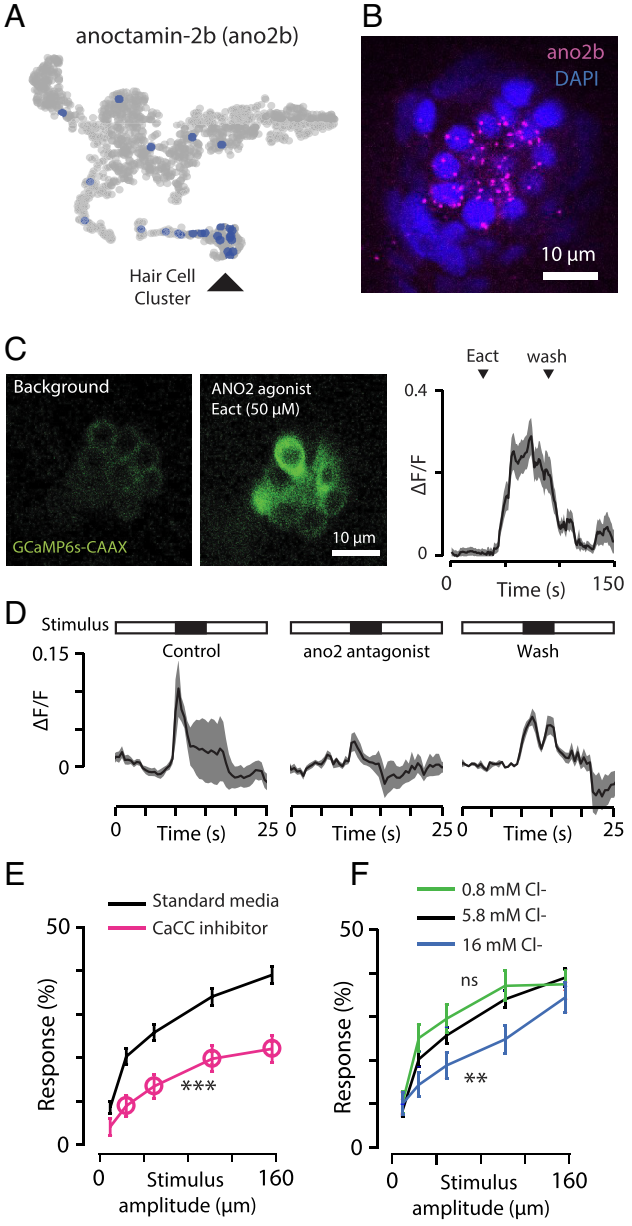

Fig. 3. Calcium-activated chloride channels are expressed in lateral line hair cells, sufficient to activate hair cells, and necessary for functional responses at the cellular and organismal level. (*A*) Visualization of single-cell transcriptome data for lateral line neuromast showing expression of anoctamin-2b (*ano2b*) in the hair cell cluster [t-SNE plot, data from (47)]. (*B*) In situ hybridization image showing *ano2b* expression in a lateral line neuromast (punctate pattern consistent with single-molecule RNA-FISH). (*C*) Response of hair cells to the Ano2 agonist Eact, recorded at the basal membrane using a genetically expressed fluorescent calcium indicator (*Left* and *Middle*: typical images, right: measured ΔF/F for introduction and washout, mean ± SEM). (*D*) Response of hair cells to cupula deflection while bathed in standard saline (control; *Left*), an Ano2 antagonist (25 μM T16Ainh; *Middle*), and after washout (*Right*; mean ± SEM). (*E*) Effect of the calcium-activated chloride channel (CaCC) inhibitor NFA on the behavioral response of zebrafish larvae to a mechanical stimulus. Asterisks indicate statistically significant differences integrated across stimulus intensities (*$P < 0.05$, **$P < 0.01$, ***$P < 0.001$), open circles represent significant pairwise comparisons ($P < 0.05$), and results are shown as mean ± SEM. (*F*) Similar to (*E*), except showing the effect of decreasing the electrochemical gradient supporting chloride efflux by increasing extracellular chloride.

To verify this expression, *ano2b* transcripts were labeled using HCR RNA-FISH. We observed *ano2b* labeling in lateral line hair cells, olfactory epithelium, and the dorsal habenula (Fig. 3*B* and *SI Appendix*, Fig. S4). The expression of anoctamin in the olfactory epithelium is consistent with similar findings in mammalian olfactory epithelium (47), and *ano2b* expression in the dorsal habenula of zebrafish has been previously reported (48).

We next examined whether calcium-activated chloride channels are capable of inducing depolarization of the lateral line hair cells. Using zebrafish larvae that express a fluorescent calcium indicator in hair cells [*myo6b:GCaMP6s-CAAX*; (21)], we recorded hair cell responses to the Anoctamin2 agonist Eact (49). This agonist induced immediate and robust increases in intracellular calcium at the basolateral membrane ($P < 0.001$, df = 58), which were reversible upon washout (Fig. 3*C*). We then recorded hair cell responses to mechanical stimulation in the presence of the Anoctamin2 antagonist $T16A_{inh}$-A01 (50). We found that this blockade produced significant reductions ($P = 0.026$, df = 24) of hair cell responses to mechanical stimuli that recovered after a washout ($P = 0.017$, df = 17; Fig. 3*D*). These responses are consistent with the hypothesis that calcium-activated anion channels contribute to mechanotransduction in the lateral line hair cells.

We then sought to determine whether these effects were reflected in the responses of an intact, behaving animal. When we examined the behavioral response of animals that had been treated with the calcium-activated chloride channel blocker niflumic acid (NFA) (51), we found that they exhibited a marked decrease in behavioral responses relative to untreated animals (48% decrease with 50 µm stimulus, omnibus $P < 0.001$, N = 30 exp/94 ctrl, Fig. 3*E*). Although interpretations of behavioral data must allow for the possibility of nonspecific effects, these results are consistent with the notion that calcium-activated Cl^- conductance supports lateral line function. We also examined the sensitivity of animals in media in which Cl^- concentrations were varied to manipulate the strength of the electrochemical gradient supporting anion efflux. We found that increasing this electrochemical gradient by reducing extracellular Cl^- (0.8 mM) produced a small increase in the response to stimuli relative to a freshwater medium (5.2 mM), although this effect was not significant (omnibus $P > 0.05$, N = 30 exp/94 ctrl, Fig. 3*F*). Conversely, we found that decreasing this gradient by increasing extracellular Cl^- (16 mM) reduced the response (27% decrease with 50 µm stimulus, omnibus $P < 0.01$, N = 30 exp/94 ctrl, Fig. 3*F*) relative to a freshwater medium. This suppression, but not termination, of lateral line sensitivity is consistent with the reversal potential still favoring anion efflux at this extracellular Cl^- concentration (Fig. 1*E*). Higher Cl^- concentrations were examined, and similar results were observed (*SI Appendix*, Fig. S3), although such salines impose a stronger osmotic stress that may complicate interpretation. Cumulatively, these results provide further support for the role of anion efflux in lateral line mechanotransduction.

A Hypothesis for Lateral Line Mechanotransduction. The MET channels in hair cells are permeable to both monovalent (K^+, Na^+) and divalent (Ca^{2+}) cations (7, 8). It has long been speculated that mechanotransduction in lateral line hair cells was mediated by cation influx through the apical membrane, similar to the inner ear. Here, we present evidence that the depolarization of lateral line hair cells is instead supported by anion efflux rather than cation influx. Although further work is required to fully establish the complete mechanotransduction pathway, our results suggest a new hypothesis: deflection of the hair cell bundle opens MET channels allowing influx of trace amounts of Ca^{2+}, which interacts with Ca^{2+}-activated Cl^- channels, leading to Cl^- efflux through the apical membrane that induces membrane depolarization (Fig. 4). Several lines of evidence support this hypothesis, including 1) the electrochemical gradient across the apical membrane is unable to support cation influx induced depolarization, 2) hair cells only require micromolar extracellular Ca^{2+} to function, 3) the hair cells express Ca^{2+}-activated Cl^- channels, 4) activating these channels induces hair cell depolarization, and 5) blocking these channels reduces the response of animals and individual hair cells to mechanosensory stimuli. This hypothesis raises many interesting new questions. It is unclear what the relative contributions of *ano2b* and other anion channels are to mechanotransduction or how the relative ion permeabilities of zebrafish lateral line MET channels affect Ca^{2+} influx and potential K^+ efflux. It is unknown how Ca^{2+} compartmentalization and basal/apical differences in Ca^{2+} concentration influence hair cell function. Future studies exploring these questions are likely to yield novel and general insights into the physiology of mechanotransduction.

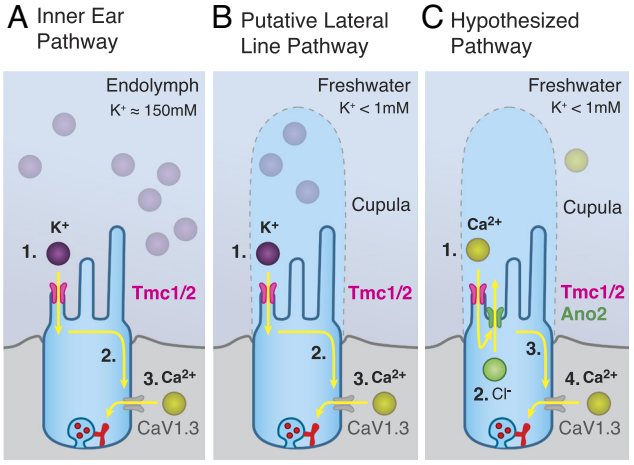

Fig. 4. Calcium-activated chloride channels amplify hair cell signaling in environments of low ionic strength. (*A*) Established inner ear pathway: Inner ear hair cells are bathed in a K^+-rich endolymph. 1. As the stereocilia deflect, mechano-electrical transduction (MET) channels open, allowing K^+ influx into the hair cells. 2. Cation influx initiates membrane depolarization. 3. Voltage-gated calcium channels allow Ca^{2+} influx at the basolateral membrane and subsequent vesicle fusion. (*B*) Putative lateral line pathway: Similar to (*A*), except the cupula encapsulating the lateral line hair cells maintains an ionic microenvironment that supports K^+ influx. (*C*) Hypothesized pathway: The apical membrane of the lateral line hair cells in zebrafish is exposed to external freshwater environments with insufficient cations to directly drive depolarization. We hypothesize that depolarization is mediated by anion efflux through the following processes: 1. Trace amounts of Ca^{2+} influx through MET channels. 2. Calcium-activated chloride channels open. 3. Cl^- efflux initiates membrane depolarization. 4. Voltage-gated calcium channels support vesicle fusion.

Discussion

Anion efflux–mediated sensory transduction provides several potential advantages for cells exposed to ion-poor environments (28). Anion efflux is expected to be robust to fluctuating external conditions, since the intracellular environment provides a well-regulated source of anions (52) and there is a strong electrochemical gradient supporting efflux across a wide range of external conditions. This intrinsic robustness could allow animals to maintain sensitivity in dynamic environments, without the need for secondary pathways for modulation or auxiliary structures that maintain a stable extracellular microenvironment. Although transduction mechanisms leveraging anion efflux have received much less attention than pathways utilizing cation influx, signal amplification through anion efflux provides an elegant solution to the challenge of fluctuating dynamic environments. This mechanism has also been found in

vertebrate olfactory receptor neurons (22–26). There, odorant receptors act via a G-protein-coupled cascade to increase cAMP, which induces opening of cyclic nucleotide-gated cation channels. This leads to an influx of Ca^{2+} and subsequent opening of Ca^{2+}-activated Cl^- channels (Ano2). This striking similarity between mechanoreceptive and olfactory systems, two apparently disparate sensory modalities, may suggest convergent evolution in systems exposed to dynamic extracorporeal environments.

The lateral line appears to have evolved in early vertebrates (12), but it is not clear whether these early vertebrates occupied marine or freshwater environments, or both at different life stages (53, 54). In a marine environment, high Na^+ and Cl^- concentrations at the apical surface would easily support cation influx–mediated depolarization and make Cl^- conductance hyperpolarizing. Here, we show that in freshwater environments, transduction would require either the establishment of an ionic microenvironment that can support cation influx or a mechanism based on anion efflux. As a result, migrations between marine and freshwater environments would be expected to have dramatic effects on lateral line function, and yet these migrations are routine for catadromous, anadromous, and euryhaline fishes. Prior studies have found that freshwater amphibians generate a K^+ microenvironment within the cupula (17, 18), while our results suggest that zebrafish larvae employ anion efflux. Understanding the evolutionary origins of lateral line hair cells and how these systems evolved as fishes and related animals entered new environments would provide important insights into hair cell physiology and the evolution of sensory systems.

The vertebrate lateral line system continues to serve as a powerful model for dissecting the basic principles of hearing and balance. However, prior studies by our labs and others have typically examined lateral line physiology in ion-rich extracellular saline that mimics vertebrate blood rather than the ion-poor saline these animals naturally inhabit (37, 55). The use of cation-rich saline would be expected to introduce an artificial cation influx while masking naturally occurring anion efflux. As such, this work highlights the necessity of studying sensory systems in the context in which they evolved in order to decipher their true properties and capacities.

Materials and Methods

Detailed methods are provided in the *SI Appendix*. Briefly, the ionic composition of the neuromast cupula was measured using ion indicators (IPG-4, ING-2, Fluo5N, BCECF, and MQAE). The sensitivity and responses to pharmacological agents of the hair cells were determined using genetically expressed fluorescent calcium indicators (myo6b:GCaMP6s-CAAX). Lastly, effects on the behavioral responses of the animals to mechanical stimuli were measured using a unique behavioral assay based on a shear-only flow stimulus.

Data, Materials, and Software Availability. All study data are included in the article and/or *SI Appendix*. The code and scripts used for analysis are available from public repositories (Neuron Image Analysis toolkit: https://bitbucket.org/jastrother/neuron_image_analysis (56), and Larval Proving Grounds toolkit: https://bitbucket.org/jastrother/larval_proving_grounds) (57).

ACKNOWLEDGMENTS. We thank K. Kindt for generously providing plasmids and transgenic zebrafish embryos, J. Ryan for his insights on transcriptome analysis, L. Desarbre for assistance with experiments, and the UF Center for Taste and Smell for its support. Funding is provided by NSF (IOS1932707 to J.A.S.; IOS1257150, IOS1855956, and IOS1856237 to J.C.L.), Paul G. Allen Frontiers Group (AGR00023117 to J.A.S.), and NIH (R01DC010809 to J.C.L.).

1. R. Fettiplace, Hair cell transduction, tuning, and synaptic transmission in the mammalian cochlea. *Compr. Physiol.* **7**, 1197–1227 (2011).
2. S. K. Bosher, R. L. Warren, Very low calcium content of cochlear endolymph, an extracellular fluid. *Nature* **273**, 377–378 (1978).
3. C. A. Smith, O. H. Lowry, M.-L. Wu, The electrolytes of the labyrinthine fluids. *Laryngoscope* **64**, 141–153 (1954).
4. B. Pan *et al.*, TMC1 and TMC2 are components of the mechanotransduction channel in hair cells of the mammalian inner ear. *Neuron* **79**, 504–515 (2013).
5. B. Pan *et al.*, TMC1 forms the pore of mechanosensory transduction channels in vertebrate inner ear hair cells. *Neuron* **99**, 736–753.e6 (2018).
6. Y. Jia *et al.*, TMC1 and TMC2 proteins are pore-forming subunits of mechanosensitive ion channels. *Neuron* **105**, 310–321.e3 (2020).
7. D. P. Corey, A. J. Hudspeth, Ionic basis of the receptor potential in a vertebrate hair cell. *Nature* **281**, 675–677 (1979).
8. H. Ohmori, Mechano-electrical transduction currents in isolated vestibular hair cells of the chick. *J. Physiol.* **359**, 189–217 (1985).
9. M. J. Dixon *et al.*, Mutation of the Na-K-Cl co-transporter gene Slc12a2 results in deafness in mice. *Hum. Mol. Genet.* **8**, 1579–1584 (1999).
10. D. C. Marcus, T. Wu, P. Wangemann, P. Kofuji, KCNJ10 (Kir4. 1) potassium channel knockout abolishes endocochlear potential. *Am. J. Physiol. Cell Physiol.* **282**, C403–C407 (2002).
11. P. Wangemann, J. Liu, D. C. Marcus, Ion transport mechanisms responsible for K+ secretion and the transepithelial voltage across marginal cells of stria vascularis in vitro. *Hearing Res.* **84**, 19–29 (1995).
12. J. M. Jørgensen, "Evolution of the octavolateralis sensory cells" in *The Mechanosensory Lateral Line*, S. Coombs, P. Görner, H. Münz, Eds. (Springer, 1989), pp. 115–145.
13. M. J. McHenry, K. E. Feitl, J. A. Strother, W. J. Van Trump, Larval zebrafish rapidly sense the water flow of a predator's strike. *Biol. Lett.* **5**, 477–479 (2009).
14. P. J. Mekdara, M. A. B. Schwalbe, L. L. Coughlin, E. D. Tytell, The effects of lateral line ablation and regeneration in schooling giant danios. *J. Exp. Biol.* **221**, jeb175166 (2018).
15. J. Olszewski, M. Haehnel, M. Taguchi, J. C. Liao, Zebrafish larvae exhibit rheotaxis and can escape a continuous suction source using their lateral line. *PLoS One* **7**, e36661 (2012).
16. A. Suli, G. M. Watson, E. W. Rubel, D. W. Raible, Rheotaxis in larval zebrafish is mediated by lateral line mechanosensory hair cells. *PLoS One* **7**, e29727 (2012).
17. F. P. McGlone, I. J. Russell, O. Sand, Measurement of calcium ion concentrations in the lateral line cupulae of Xenopus laevis. *J. Exp. Biol.* **83**, 123–130 (1979).
18. I. J. Russell, P. M. Sellick, Measurement of potassium and chloride ion concentrations in the cupulae of the lateral lines of Xenopus laevis. *J. Physiol.* **257**, 245–255 (1976).
19. T. Nicolson *et al.*, Genetic analysis of vertebrate sensory hair cell mechanosensation: The zebrafish circler mutants. *Neuron* **20**, 271–283 (1998).
20. A. J. Ricci *et al.*, Patch-clamp recordings from lateral line neuromast hair cells of the living zebrafish. *J. Neurosci.* **33**, 3131–3134 (2013).
21. Q. Zhang *et al.*, Synaptically silent sensory hair cells in zebrafish are recruited after damage. *Nat. Commun.* **9**, 1–16 (2018).
22. A. B. Stephan *et al.*, ANO2 is the cilial calcium-activated chloride channel that may mediate olfactory amplification. *Proc. Natl. Acad. Sci. U.S.A.* **106**, 11776–11781 (2009).
23. S. J. Kleene, R. C. Gesteland, Calcium-activated chloride conductance in frog olfactory cilia. *J. Neurosci.* **11**, 3624–3629 (1991).
24. G. Lowe, G. H. Gold, Nonlinear amplification by calcium-dependent chloride channels in olfactory receptor cells. *Nature* **366**, 283–286 (1993).
25. A. P. Cherkashin *et al.*, Expression of calcium-activated chloride channels Ano1 and Ano2 in mouse taste cells. *Pflugers Arch – Eur. J. Physiol.* **468**, 305–319 (2016).
26. J. Reisert, J. Lai, K.-W. Yau, J. Bradley, Mechanism of the excitatory Cl- response in mouse olfactory receptor neurons. *Neuron* **45**, 553–561 (2005).
27. T. Kurahashi, K.-W. Yau, Olfactory transduction: Tale of an unusual chloride current. *Curr. Biol.* **4**, 256–258 (1994).
28. J. Reisert, J. Reingruber, Ca2+-activated Cl- current ensures robust and reliable signal amplification in vertebrate olfactory receptor neurons. *Proc. Natl. Acad. Sci. U.S.A.* **116**, 1053–1058 (2019).
29. R. Spence, G. Gerlach, C. Lawrence, C. Smith, The behaviour and ecology of the zebrafish, Danio rerio. *Biol. Rev.* **83**, 13–34 (2008).
30. R. Spence *et al.*, The distribution and habitat preferences of the zebrafish in Bangladesh. *J. Fish Biol.* **69**, 1435–1448 (2006).
31. M. M. Sarin, S. Krishnaswami, Major ion chemistry of the Ganga-Brahmaputra river systems, India. *Nature* **312**, 538–541 (1984).
32. A. Brandt, D. Khimich, T. Moser, Few CaV1.3 channels regulate the exocytosis of a synaptic vesicle at the hair cell ribbon synapse. *J. Neurosci.* **25**, 11577–11585 (2005).
33. B. S. Dezfuli, S. Magosso, E. Simoni, K. Hills, R. Berti, Ultrastructure and distribution of superficial neuromasts of blind cavefish, Phreatichthys andruzzii, juveniles. *Microscopy Res. Technique* **72**, 665–671 (2009).
34. Å. Flock, J. M. Jørgensen, The ultrastructure of lateral line sense organs in the juvenile salamander Ambystoma mexicanum. *Cell Tissue Res.* **152**, 283–292 (1974).
35. A. L. Hodgkin, A. F. Huxley, A quantitative description of membrane current and its application to conduction and excitation in nerve. *J. Physiol.* **117**, 500–544 (1952).
36. M. Beurg, J.-H. Nam, A. Crawford, R. Fettiplace, The actions of calcium on hair bundle mechanics in mammalian cochlear hair cells. *Biophys. J.* **94**, 2639–2653 (2008).
37. J. Olt, S. L. Johnson, W. Marcotti, In vivo and in vitro biophysical properties of hair cells from the lateral line and inner ear of developing and adult zebrafish. *J. Physiol.* **592**, 2041–2058 (2014).
38. J. Peloggia *et al.*, Adaptive cell invasion maintains lateral line organ homeostasis in response to environmental changes. *Dev. Cell* **56**, 1296–1312 (2021).
39. O. Sand, Effects of different ionic environments on the mechano-sensitivity of lateral line organs in the mudpuppy. *J. Comp. Physiol.* **102**, 27–42 (1975).
40. A. B. Coffin, K. E. Reinhart, K. N. Owens, D. W. Raible, E. W. Rubel, Extracellular divalent cations modulate aminoglycoside-induced hair cell death in the zebrafish lateral line. *Hearing Res.* **253**, 42–51 (2009).
41. M. Beurg, M. G. Evans, C. M. Hackney, R. Fettiplace, A large-conductance calcium-selective mechanotransducer channel in mammalian cochlear hair cells. *J. Neurosci.* **26**, 10992–11000 (2006).

42. V. Di Donato, T. O. Auer, K. Duroure, F. Del Bene, Characterization of the calcium binding protein family in zebrafish. *PLoS One* **8**, e53299 (2013).
43. A. J. Ricci, A. C. Crawford, R. Fettiplace, Tonotopic variation in the conductance of the hair cell mechanotransducer channel. *Neuron* **40**, 983–990 (2003).
44. M. J. McHenry, J. A. Strother, S. M. Van Netten, Mechanical filtering by the boundary layer and fluid–structure interaction in the superficial neuromast of the fish lateral line system. *J. Comp. Physiol. A* **194**, 795 (2008).
45. H. E. Karlsen, O. Sand, Selective and reversible blocking of the lateral line in freshwater fish. *J. Exp. Biol.* **133**, 249–262 (1987).
46. M. E. Lush *et al.*, scRNA-Seq reveals distinct stem cell populations that drive hair cell regeneration after loss of Fgf and Notch signaling. *Elife* **8**, e44431 (2019).
47. S. Rasche *et al.*, Tmem16b is specifically expressed in the cilia of olfactory sensory neurons. *Chem. Senses* **35**, 239–245 (2010).
48. T. N. deCarvalho *et al.*, Neurotransmitter map of the asymmetric dorsal habenular nuclei of zebrafish. *Genesis* **52**, 636–655 (2014).
49. W. Namkung, Z. Yao, W. E. Finkbeiner, A. S. Verkman, Small-molecule activators of TMEM16A, a calcium-activated chloride channel, stimulate epithelial chloride secretion and intestinal contraction. *FASEB J.* **25**, 4048–4062 (2011).
50. W. Namkung, P.-W. Phuan, A. S. Verkman, TMEM16A inhibitors reveal TMEM16A as a minor component of calcium-activated chloride channel conductance in airway and intestinal epithelial cells*. *J. Biol. Chem.* **286**, 2365–2374 (2011).
51. S. Pifferi, M. Dibattista, A. Menini, TMEM16B induces chloride currents activated by calcium in mammalian cells. *Pflügers Archiv-Eur. J. Physiol.* **458**, 1023–1038 (2009).
52. K. Kaila, T. J. Price, J. A. Payne, M. Puskarjov, J. Voipio, Cation-chloride cotransporters in neuronal development, plasticity and disease. *Nat. Rev. Neurosci.* **15**, 637–654 (2014).
53. R. W. Griffith, Freshwater or marine origin of the vertebrates? *Comp. Biochem. Physiol. Part A Physiol.* **87**, 523–531 (1987).
54. L. B. Halstead, W. G. Chaloner, J. D. Lawson, The vertebrate invasion of fresh water. *Philos. Trans. R. Soc. London B Biol. Sci.* **309**, 243–258 (1985).
55. E. T. Lunsford, D. A. Skandalis, J. C. Liao, Efferent modulation of spontaneous lateral line activity during and after zebrafish motor commands. *J. Neurophysiol.* **122**, 2438–2448 (2019).
56. J. A. Strother, Neuron Image Analysis Toolkit. Bitbucket.org. https://bitbucket.org/jastrother/neuron_image_analysis/. Deposited 20 April 2022.
57. J. A. Strother, Larval Proving Grounds Toolkit. Bitbucket.org. https://bitbucket.org/jastrother/larval_proving_grounds/. Deposited 12 May 2023.